

Article

A New Practice to Monitor the Fabrication Process of Fab-Targeting Ligands from Bevacizumab by LC-MS: Preparation and Analytical Characterization

Franck Marquet ^{1,2} , Valentina D'Atri ^{1,2} , Davy Guillarme ^{1,2,*} and Gerrit Borchard ^{1,2,*} 

¹ Section of Pharmaceutical Sciences, University of Geneva, CMU—Rue Michel-Servet 1, 1211 Geneva, Switzerland; Franck.Marquet@unige.ch (F.M.); Valentina.Datri@unige.ch (V.D.)

² Institute of Pharmaceutical Sciences of Western Switzerland (ISPSO), University of Geneva, CMU—Rue Michel-Servet 1, 1211 Geneva, Switzerland

* Correspondence: Davy.Guillarme@unige.ch (D.G.); Gerrit.Borchard@unige.ch (G.B.)

Abstract: The objective of this study was to qualitatively evaluate a Fab-targeting ligand preparation containing free thiol groups in the hinge region by using bevacizumab as a model. The evaluation focused on the purification of fragments through a nonaffinity-based process using a centrifugal ultrafiltration technique and mild reduction conditions for the intact production of F(ab') fragments with specific inter-heavy-chain disulfide bonds cleavage. Under these conditions, F(ab') fragments with a defined chemical composition were successfully obtained via proteolytic digestion followed by a controlled reduction reaction process maintaining the integrity of the binding sites. The ultrafiltration purification technique appears to be suitable for the removal of the digestive enzyme but inefficient for the removal of Fc fragments, thus requiring additional processing. A suitable analytical strategy was developed, allowing us to demonstrate the reformation of disulfide bridges between the two reduced cysteines within F(ab') fragments.

Keywords: antibody–drug conjugate (ADC); site-specific conjugation; high-resolution mass spectrometry; thiol–maleimide “click” chemistry; targeted nanomedicine



Citation: Marquet, F.; D'Atri, V.; Guillarme, D.; Borchard, G. A New Practice to Monitor the Fabrication Process of Fab-Targeting Ligands from Bevacizumab by LC-MS: Preparation and Analytical Characterization. *Sci. Pharm.* **2022**, *90*, 5. <https://doi.org/10.3390/scipharm90010005>

Academic Editor: Helen D. Skaltsa

Received: 1 November 2021

Accepted: 21 December 2021

Published: 4 January 2022

Publisher's Note: MDPI stays neutral with regard to jurisdictional claims in published maps and institutional affiliations.



Copyright: © 2022 by the authors. Licensee MDPI, Basel, Switzerland. This article is an open access article distributed under the terms and conditions of the Creative Commons Attribution (CC BY) license (<https://creativecommons.org/licenses/by/4.0/>).

1. Introduction

An interesting way of decorating nanomedicines, which can home in on targeted cells, is to examine how targeted drug delivery was first developed in the form of an antibody–drug conjugate (ADC). ADCs consist of one or several molecules of a highly cytotoxic compound covalently bound to an antibody, which can target cancer cells. Only in 1983 the scientific concept of a “Zauberkegel” (magic bullet) envisioned by Paul Ehrlich at the beginning of the 20th century had been realized in clinical application of this biochemical platform [1]. This approach represents an excellent starting point for the engineering of targeted nanoparticles.

Modalities of conjugation to antibody molecules are achieved through several suitable functional groups. Amide coupling, connecting a payload to a lysine residue, is one of the most reliable and high-yielding chemical conversions of antibody conjugation [2]. Nonetheless, this conventional conjugation procedure can lead to random crosslinking. Due to the abundance of amine and carboxylate groups throughout the surface topology of an antibody, their conjugations can lead to a possible obscuration of the antigen-binding site, thus reducing targeting activity [3]. Amide coupling, while feasible, as in the case of the first ADC approved by the FDA for the indication of solid tumors (Kadcyla[®], Genentech, Inc., San Francisco, CA, USA) [4], requires reproducible manufacturing processes [2]. Due to the abundant chemical access of lysine residues on the antibody structure, it may often result in products of heterogeneous molecular weight, molecular species with variable conjugation sites and drug-to-antibody ratios (DAR).

With proper knowledge of the monoclonal antibody (mAb) structure, a polymeric conjugation may be oriented to avoid impeding the antigen recognition at the binding site. More defined cysteine-based conjugation is thus considered to be superior. The disulfides in the hinge region that connect the heavy chains can be selectively cleaved by reducing agents. For example, the construction of commercial ADC Adcetris[®] (Seagen, Inc., Bothell, WA, USA) comprises on average four molecules of monomethyl auristatin E (MMAE) toxin attached to cAC10 interchain cysteine residues through the protease-cleavable Val-Cit-p-amino-benzyloxycarbon (PABC) linker [5]. Proteolytic digestion is used for the separation of the Fc region and the formation of Fab fragments (Figure 1). As systemic administration is the most frequent route for cancer treatment, the reticuloendothelial system (RES), a major barrier in cancer nanomedicine, needs to be avoided [3]. Through Fc region removal, which is more likely to interact with the immune system [6], a benefit of decoration by F(ab') fragments is suggested to improve the pharmacokinetic properties of targeted nanoparticles.

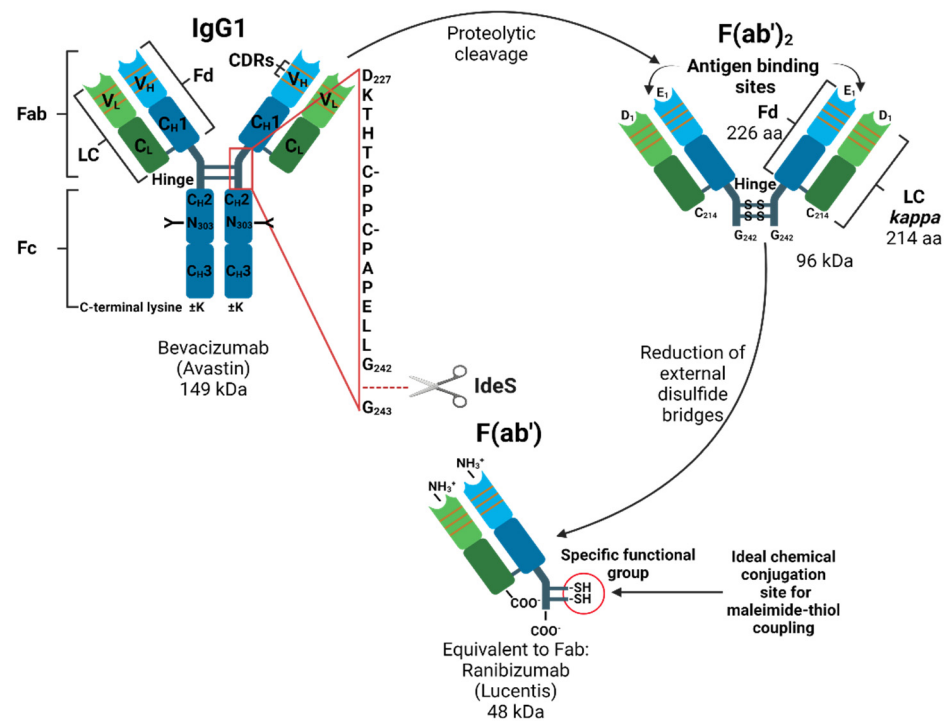


Figure 1. Schematic overview of the preparation of Fab-targeting ligands. Bevacizumab, a human immunoglobulin G (IgG1) is presented with a zoom on the hinge region indicating the cleavage site of *IdeS* protease, adapted from [7]. The heavy chains (HC) contain one variable domain (V_L) and three constant domains (C_H1-C_H3). The light chain (LC) has one constant domain (C_L) and one variable domain (V_L) classified as *kappa*. Fd is the heavy chain portion of Fab consisting of (V_H-C_H1). Variable domains (V_L-V_H) of light and heavy chains contain murine complementarity-determining regions (CDRs) [8]. The fragment crystallizable (Fc) consists of two constant domains (C_H2-C_H3). Biantennary oligosaccharides (Y) are linked through the N-glycosylation site via asparagine (N₃₀₃) residue located in the C_H2 domain [9]. F(ab')₂ has two antigen-binding sites linked together by disulfide bonds and is generated by removing the Fc region while leaving the hinge region intact. The F(ab') fragment is monovalent and generated by a mild reduction of the F(ab')₂ fragment. Amino acids (aa) are presented with a single letter code and numbered according to the Kabat numbering scheme [10].

For this purpose, a Fab-targeting ligand preparation route (Figure 1) was followed, enabling exhibition of thiol functional groups for selective coupling of a maleimide functional

moiety. Bevacizumab was selected as a model antibody for the preparation of ligands for potential successive preparation of targeted nanoparticle.

In contrast to the *N*-glycosylated full-length mAb bevacizumab (Avastin[®], Genentech, Inc., San Francisco, CA, USA), which is produced in eukaryotic cells of the Chinese hamster ovary (CHO), the non-glycosylated ranibizumab (Lucentis[®], Genentech, Inc., San Francisco, CA, USA) is produced in prokaryotic *Escherichia coli* by recombinant DNA technology [11,12]. The goal of this project was to evaluate a rapid F(ab')-targeting ligand preparation through the use of a protease that specifically cleaves a unique site below the hinge region and to evaluate the downstream purification process through an inexpensive method using centrifugal ultrafiltration.

2. Materials and Methods

2.1. Materials

Vials of bevacizumab (Avastin[®], Genentech, Inc., San Francisco, CA, USA) 25 mg/mL were kindly provided by the Hospital Pharmacy of the University Hospitals of Geneva (Geneva, Switzerland). FabRICATOR[®] (*IdeS* protease) was obtained from Genovis AB (Lund, Sweden). β -Mercaptoethanol (β -MEA), DL-dithiothreitol (DTT), ethylenediaminetetraacetic acid disodium salt (EDTA), Hydrochloric acid fuming $\geq 37\%$ (HCl), tris-hydroxymethyl-aminomethane (TRIS), formic acid (FA $\geq 99\%$), and trifluoroacetic acid (TFA $\geq 99\%$) were purchased from Sigma-Aldrich (St Louis, MO, USA). UHPLC-MS grade acetonitrile (ACN) and water were supplied by Biosolve (Valkenswaard, The Netherlands).

2.2. Enzymatic Digests and Sample Preparation

Bevacizumab was diluted from the stock solution to a concentration of 1 mg/mL (100 μ g) in 10 mM TRIS buffer pH 7.2. The drug product was then digested with 100 units of *IdeS* enzyme FabRICATOR[®] (Genovis AB, Lund, Sweden) in a final volume of 100 μ L of TRIS 100 mM, adjusted to pH 7.2 with 1 M HCl. After 30 min incubation at 45 °C, samples were purified and concentrated three times at room temperature by centrifugal ultrafiltration at 10,000 \times g for 5 min using Vivaspin[®] 500 (50 kDa) (Sartorius, Göttingen, Germany). Samples were then reduced by DTT 10 mM for 30 min at room temperature. Another optimized reducing procedure was carried out at room temperature for 30 min by β -MEA 10 mM in 5 mM EDTA, as previously published [13]. Removal of reducing agents was carried out by centrifugal ultrafiltration using Vivaspin[®] 500 (10 kDa) (Sartorius, Göttingen, Germany) under the aforementioned conditions.

2.3. Chromatographic System

Digested samples were analyzed by LC-MS as previously described [14]. Briefly, an Acquity UPLC system (Waters, Milford, MA, USA) equipped with a binary solvent delivery pump and autosampler was coupled to a fluorescence detector (FD), and an electrospray time-of-flight mass spectrometer (Waters Xevo[™] Q-ToF). A Waters Acquity UPLC Protein BEH C4 chromatographic column (300 Å, 1.7 μ m, 2.1 mm \times 150 mm) was mounted on the instrument for the analysis. FD data were acquired at 280 nm excitation and 360 nm emission wavelengths with a 5 Hz sampling rate at 0.4 s time constant. The mass spectrometer was operated in the positive ion mode and ions were scanned over *m/z* 1000–4000 using a scan rate of 1 s. The capillary voltage was set to 3.0 kV, sample cone voltage of 30 V, source temperature to 150 °C, desolvation gas temperature to 500 °C, and gas flow to 1000 L/h. Mobile phase A was 0.08% TFA and 0.02% FA in water and mobile phase B was 0.08% TFA and 0.02% FA in ACN. A linear gradient from 28 to 42% B in 12 min was run, followed by 1 min wash at 70% B and 5 min re-equilibration. The flow rate was set to 0.4 mL/min and the column temperature to 80 °C. The injection volume was set to 1 μ L. Data acquisition and analysis were performed with MassLynx V4.1 (Waters, Milford, MA, USA).

3. Results

The process consisted of three stages. First, digestion of IgG1 into Fc/2 (25 kDa) and F(ab')₂ was carried out within minutes. Second, the removal of Fc/2 by centrifugal ultrafiltration at a sizable cutoff of 50 kDa was investigated. Finally, two mild reduction conditions were tested in order to maintain the integrity of the binding sites of the F(ab') fragments. The proteolytic cleavage of bevacizumab into 2 × Fc/2 and F(ab')₂ is observed by reverse-phase liquid chromatography (RPLC) fluorescence chromatogram (Figure 2). The fluorescent signals as a result of a reduction of external disulfide bridges of F(ab')₂ into 2 × F(ab') by mild reduction conditions are also shown.

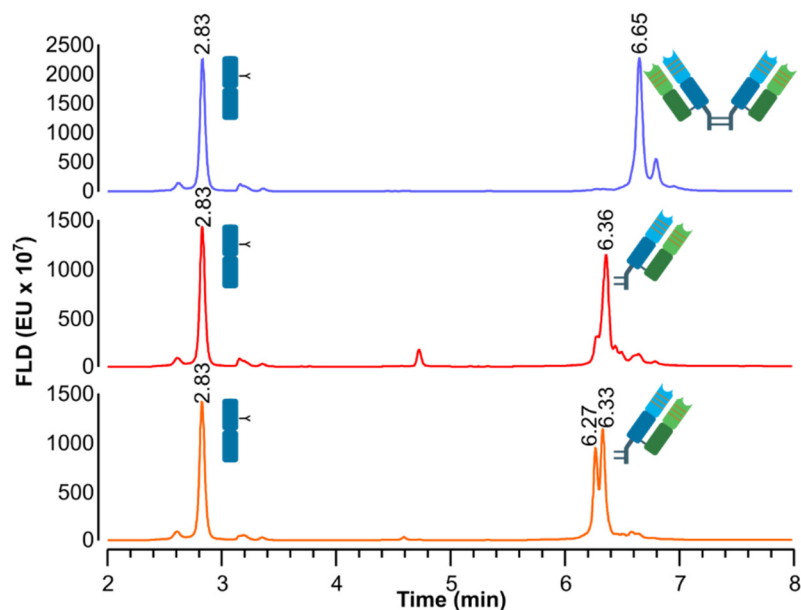


Figure 2. RPLC fluorescence chromatograms of *IdeS*-digested bevacizumab (blue), *IdeS*-digested bevacizumab, reduced with DTT (red) and *IdeS*-digested bevacizumab, reduced with β -MEA (orange).

The presence of *IdeS* enzyme (37 kDa) was not observed, demonstrating the efficiency of the purification method by Vivaspin[®] ultrafiltration. However, Fc/2 fragments were detected on chromatograms, indicating that other purification methods must be used.

The presence of Fc/2 fragments was confirmed by MS assignment (Figure 3).

Two peaks with different masses were detected as observed on the deconvoluted MS spectrum (Figure 3B), and attributed to two major complex bisecting glycan structures. Two core-fucosylated (F) *N*-linked glycans with either zero (G0) or one (G1) terminal galactose residue, presented as glycosylation G0F and G1F, were identified with a predominant (G0F) glycoform, as highlighted by an experimental mass shift of 162.88 Da. This result is consistent with a galactose theoretical mass shift of 162.14 Da, as previously shown by denaturing chromatography hyphenated to mass spectrometry [15]. Without the addition of reducing agents, the disulfide bonds in the hinge region maintain the two Fab fragments in one entity of approximately 100 kDa, as shown in Figure 3C.

After demonstrating a successful proteolytic cleavage, the reduction of F(ab')₂ into 2 × F(ab') was confirmed by MS assignment (Figure 4). The examination of cysteines (free vs. linked) located at the hinge region was carefully conducted.

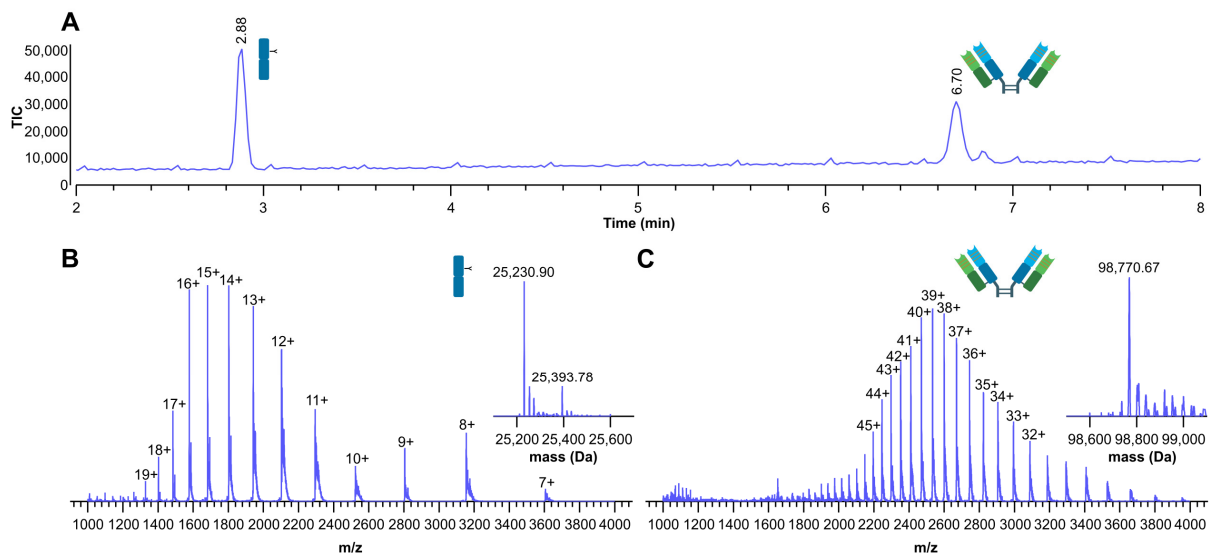


Figure 3. (A) Total ion chromatogram (TIC) of *IdeS* digested bevacizumab; (B) deconvoluted and multi-charged ions MS spectra with the assignments of Fc/2; (C) deconvoluted and multi-charged ions MS spectra with the assignment of F(ab')₂.

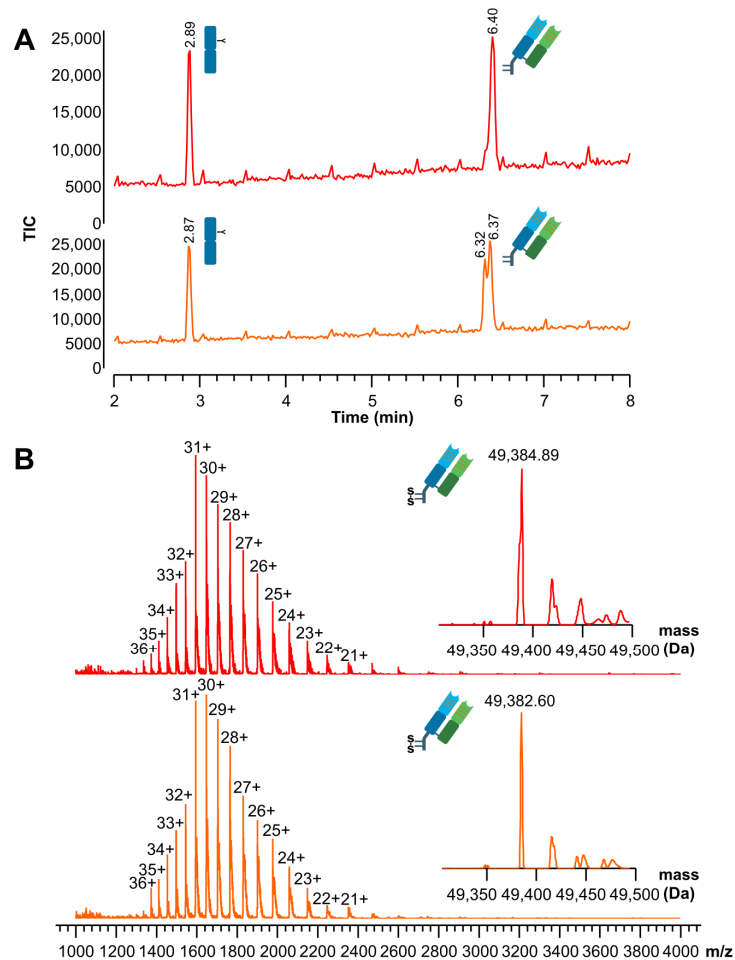


Figure 4. (A) Total ion chromatograms (TIC) of *IdeS* digested bevacizumab, dialyzed and reduced by DTT (red) or β -MEA (orange); (B) MS spectra with the assignment of F(ab')₁, reduced by DTT (red) and reduced by β -MEA (orange).

Results show a reduction of F(ab')₂ into 2 × F(ab') by DTT and β-MEA, respectively, with MS assignments of reduced fragments. Intra-hinge disulfide bond reformation appears to occur after reduction under mild conditions. Table 1 lists detailed mass assignments obtained through these procedures.

Table 1. Fragments retention times and mass assignments performed by RPLC-MS.

Samples	t _r (Min)	Assignment	Theoretical Masses (Da) ¹	Experimental Masses (Da)	Δm (Da)	ppm (Error)
<i>IdeS</i> -digested bevacizumab	2.88	Fc/2-K G0F	25,232.28	25,230.90	1.38	55
	6.70	Fc/2-K G1F	25,394.42	25,393.78	0.64	25
		F(ab') ₂	98,770.35	98,770.67	−0.32	−3
<i>IdeS</i> -digested bevacizumab, reduced by DTT	2.89	Fc/2-K G0F	25,232.28	25,231.83	0.45	18
	6.40	Fc/2-K G1F	25,394.42	25,393.37	1.05	41
		Fab (Cys. linked)	49,385.18	49,384.89	0.29	6
<i>IdeS</i> -digested bevacizumab, reduced by β-MEA	2.87	Fc/2-K G0F	25,232.28	25,231.12	1.16	46
	6.32	Fc/2-K G1F	25,394.42	25,393.26	1.16	46
		Fab (Cys. linked)	49,385.18	49,383.43	1.75	35
	6.37	Fab (Cys. linked)	49,385.18	49,382.80	2.38	48

¹ Theoretical masses have been generated by the MS software considering an intra-hinge disulfide bond of F(ab').

4. Discussion

Both tested conditions were suitable for selectively cleaving *hinge-region* disulfide bonds by splitting the F(ab')₂ into two univalent F(ab') fragments without affecting the intrachain disulfide bonds between light chains and the heavy-chain portion of Fab. Interestingly, it can be assumed that the two cysteines normally involved in pairing the heavy chains did not remain in the reduced form, suggesting the formation of an intra-hinge disulfide bond. Indeed, we observed that the molecular weight obtained (49,383 Da) was quite far from the theoretical molecular weight of Fab containing sulfhydryl groups (49,387 Da) compared to the theoretical molecular weight of Fab leaving no single cysteine in the reduced form (49,385 Da).

Among the physicochemical properties of mAbs, the isoelectric point (*pI*) [16] as well as their hydrophobicity [17] must be considered. Although the Fc fragment is well degraded, this subunit cannot be carefully separated by simple filtration. One probable explanation is that *IdeS* cleaves in a region that contains a high density of hydrophobic residues. Moreover, bevacizumab is known to be hydrophobic, as reflected by its high retention factor (*k* = 4.3) in hydrophobic interaction chromatography (HIC) [17]. This hydrophobic behavior has been recently demonstrated by a purely physics-based method predicting a localized description of the free energy of hydration allowing visualization of a large hydrophobic region at the complementarity-determining regions (CDRs) strongly depending on the protein conformation [18]. Producing fragments with a high terminal density of hydrophobic residues could ultimately lead to agglomerates of larger molecular weights due to noncovalent interactions. Moreover, Vivaspin[®] filtration membranes are made of polyethersulfone (PES), which is particularly hydrophobic and may be a reason for membrane biofouling [19]. The hydrophobic surface of PES is a serious limitation to the use of Vivaspin[®] ultrafiltration units as a purification process resulting in a poor separation performance of mAbs fragments. In addition, repeated use may lead to an undesirable accumulation of Fc fragments resulting in blocked membranes.

Purification by other approaches such as affinity-based processes should therefore be considered. The initial goal was to investigate the cleavage of F(ab')₂ by using *IdeS* endopeptidase and characterization of the obtained fragments. Other methods for the separation of Fc and F(ab') fragments were not implemented but are briefly detailed below.

One of the advantages of using *IdeS* is the rapid digestion within minutes (30 min) compared to several hours (12 h) for pepsin protease [13]. With the advantage of enhanced digestion of the Fc part resulting in many small Fc fragments, pepsin digestion could be explored and combined with the ultrafiltration process. Several processing alternatives

exist for mAb fragment purification, without the emergence of a method of choice [20]. An ideal purification method should be rapid, high-yield, and generically applicable for a wide range of Ab fragments [20,21]. For *IdeS* digestion, protein-based affinity chromatography can be applied as it provides purification options assigned to unique binding sites, thus reducing downstream process development efforts for each fragment under consideration and often resulting in higher one-step purity and yield. For example, antibody-binding proteins isolated from the cell wall surface of bacteria, such as protein A, a 42 kDa protein from *Staphylococcus aureus* [22] is a ligand applicable for the purification of human IgG1, 2, and 4 formats [20]. This protein is usually immobilized onto a solid support to create an affinity matrix that can be used in a column format. The primary binding site of protein A on IgG is situated at the junction between the C_H2 and C_H3 on the Fc fragment without affecting the antigen-binding site [23], and should therefore be optimal to intercept intact Fc/2 and properly sieve targeting ligands. Other unknown “hot-spots” for specific binding at the hinge between V_H and C_H1 domains of Fab were suggested by a molecular docking approach [24]. The proteins’ A-based affinity media are most frequently used to purify full-size antibodies, showing that purification of antibody fragments (Fabs) from *E. coli* crude extracts is more challenging in comparison to the purification of the whole molecule. For this purpose, other antibody-binding proteins, e.g., protein L present on the surface of *Peptostreptococcus magnus* can be employed. This protein possesses strong affinity binding on *Kappa* light chains 1, 2, and 4, as well as Fab, ScFv, and dAb fragments, but has no affinity for *Lambda* light chain [20].

5. Conclusions

In this study, the preparation of Fab targeting ligands was explored using bevacizumab as an IgG model through a unique specific cleavage and under two different mild reduction conditions. Centrifugal ultrafiltration was used as a purification process and LC-MS as an analytical tool to determine the nature of generated fragments. Reductant solutions with two different reducing agents, namely DTT and β -MEA, were tested, demonstrating the successful formation of Fab fragments containing intra-hinge disulfide bonds. The centrifugal ultrafiltration process was found to be unsuitable to remove Fc fragments, despite a significant difference in molecular weights between Fc/2 and F(ab')₂ fragments.

Although adjustments are still necessary for the purification process in view of site-specific conjugation preparation strategy, the analytical method employed in the present study showed very high reliability in monitoring the preparation of targeting protein ligands. LC-MS can therefore be successfully employed as a monitoring tool in the fabrication process of targeting moieties for use in nanomedicines. We believe that the attachment of targeting ligands, as well as their proper orientation, can be finely controlled using this methodology. High-resolution mass spectrometry should be further considered to quantify the number of ligands present on a colloidal drug delivery vector, as this critical quality attribute can be regarded as a presage of performance by influence on the prolonged circulation time and the targetability through the specific binding to targeted cells.

Author Contributions: Conceptualization, F.M.; methodology, V.D.; validation, V.D. and D.G.; formal analysis, F.M. and V.D.; investigation, F.M.; resources, V.D. and D.G.; data curation, V.D. and D.G.; writing—original draft preparation, F.M.; writing—review and editing, F.M., V.D., D.G. and G.B.; visualization, F.M. and V.D.; supervision, V.D.; project administration, G.B.; funding acquisition, G.B. All authors have read and agreed to the published version of the manuscript.

Funding: This work was supported by a grant from the Swiss National Science Foundation (project ID 200021_157033).

Acknowledgments: The authors are grateful to Sandrine Fleury-Souverain for providing us with samples of the monoclonal antibody.

Conflicts of Interest: The authors declare no conflict of interest.

References

1. Ford, C.H.; Newman, C.E.; Johnson, J.R.; Woodhouse, C.S.; Reeder, T.A.; Rowland, G.F.; Simmonds, R.G. Localisation and toxicity study of a vindesine-anti-CEA conjugate in patients with advanced cancer. *Br. J. Cancer* **1983**, *47*, 35–42. [[CrossRef](#)] [[PubMed](#)]
2. Tsuchikama, K.; An, Z. Antibody-drug conjugates: Recent advances in conjugation and linker chemistries. *Protein Cell* **2018**, *9*, 33–46. [[CrossRef](#)] [[PubMed](#)]
3. Manjappa, A.S.; Chaudhari, K.R.; Venkataraju, M.P.; Dantuluri, P.; Nanda, B.; Sidda, C.; Sawant, K.K.; Murthy, R.S. Antibody derivatization and conjugation strategies: Application in preparation of stealth immunoliposome to target chemotherapeutics to tumor. *J. Control. Release* **2011**, *150*, 2–22. [[CrossRef](#)]
4. Birrer, M.J.; Moore, K.N.; Betella, I.; Bates, R.C. Antibody-drug conjugate-based therapeutics: State of the science. *J. Natl. Cancer Inst.* **2019**, *111*, 538–549. [[CrossRef](#)] [[PubMed](#)]
5. Senter, P.D.; Sievers, E.L. The discovery and development of brentuximab vedotin for use in relapsed Hodgkin lymphoma and systemic anaplastic large cell lymphoma. *Nat. Biotechnol.* **2012**, *30*, 631–637. [[CrossRef](#)]
6. Kedmi, R.; Veiga, N.; Ramishetti, S.; Goldsmith, M.; Rosenblum, D.; Dammes, N.; Hazan-Halevy, I.; Nahary, L.; Leviatan-Ben-Arye, S.; Harlev, M.; et al. A modular platform for targeted RNAi therapeutics. *Nat. Nanotechnol.* **2018**, *13*, 214–219. [[CrossRef](#)]
7. Lippold, S.; Nicolardi, S.; Wuhler, M.; Falck, D. Proteoform-resolved FcRIIIa binding assay for Fab glycosylated monoclonal antibodies achieved by affinity chromatography mass spectrometry of Fc moieties. *Front. Chem.* **2019**, *7*, 698. [[CrossRef](#)]
8. Presta, L.G.; Chen, H.; O'Connor, S.J.; Chisholm, V.; Meng, Y.G.; Krummen, L.; Winkler, M.; Ferrara, N. Humanization of an anti-vascular endothelial growth factor monoclonal antibody for the therapy of solid tumors and other disorders. *Cancer Res.* **1997**, *57*, 4593–4599.
9. Seo, N.; Polozova, A.; Zhang, M.; Yates, Z.; Cao, S.; Li, H.; Kuhns, S.; Maher, G.; McBride, H.J.; Liu, J. Analytical and functional similarity of Amgen biosimilar ABP 215 to bevacizumab. *MAbs* **2018**, *10*, 678–691. [[CrossRef](#)]
10. Kabat, E.A.; Wu, T.T.; Perry, H.; Gottesman, K.; Foeller, C. *Sequences of Proteins of Immunological Interest*, 5th ed.; NIH Publication No. 91-3242; NIH: Bethesda, MD, USA, 1991.
11. Steinbrook, R. The price of sight—ranibizumab, bevacizumab, and the treatment of macular degeneration. *N. Engl. J. Med.* **2006**, *355*, 1409–1412. [[CrossRef](#)]
12. Plyukhova, A.A.; Budzinskaya, M.V.; Starostin, K.M.; Rejdak, R.; Bucolo, C.; Reibaldi, M.; Toro, M.D. Comparative safety of bevacizumab, ranibizumab, and aflibercept for treatment of neovascular age-related macular degeneration (AMD): A systematic review and network meta-analysis of direct comparative studies. *J. Clin. Med.* **2020**, *9*, 1522. [[CrossRef](#)]
13. Zhou, Z.; Zhang, J.; Zhang, Y.; Ma, G.; Su, Z. Specific conjugation of the hinge region for homogeneous preparation of antibody fragment-drug conjugate: A case study for doxorubicin-PEG-anti-CD20 Fab' synthesis. *Bioconjug. Chem.* **2016**, *27*, 238–246. [[CrossRef](#)] [[PubMed](#)]
14. D'Atri, V.; Fekete, S.; Stoll, D.; Lauber, M.; Beck, A.; Guillaume, D. Characterization of an antibody-drug conjugate by hydrophilic interaction chromatography coupled to mass spectrometry. *J. Chromatogr. B Analyt. Technol. Biomed. Life Sci.* **2018**, *1080*, 37–41. [[CrossRef](#)] [[PubMed](#)]
15. D'Atri, V.; Goyon, A.; Bobaly, B.; Beck, A.; Fekete, S.; Guillaume, D. Protocols for the analytical characterization of therapeutic monoclonal antibodies. III—Denaturing chromatographic techniques hyphenated to mass spectrometry. *J. Chromatogr. B Analyt. Technol. Biomed. Life Sci.* **2018**, *1096*, 95–106. [[CrossRef](#)]
16. Goyon, A.; Excoffier, M.; Janin-Bussat, M.C.; Bobaly, B.; Fekete, S.; Guillaume, D.; Beck, A. Determination of isoelectric points and relative charge variants of 23 therapeutic monoclonal antibodies. *J. Chromatogr. B Analyt. Technol. Biomed. Life Sci.* **2017**, *1065–1066*, 119–128. [[CrossRef](#)] [[PubMed](#)]
17. Goyon, A.; D'Atri, V.; Colas, O.; Fekete, S.; Beck, A.; Guillaume, D. Characterization of 30 therapeutic antibodies and related products by size exclusion chromatography: Feasibility assessment for future mass spectrometry hyphenation. *J. Chromatogr. B Analyt. Technol. Biomed. Life Sci.* **2017**, *1065–1066*, 35–43. [[CrossRef](#)]
18. Waibl, F.; Fernandez-Quintero, M.L.; Kamenik, A.S.; Kraml, J.; Hofer, F.; Kettenberger, H.; Georges, G.; Liedl, K.R. Conformational ensembles of antibodies determine their hydrophobicity. *Biophys. J.* **2021**, *120*, 143–157. [[CrossRef](#)] [[PubMed](#)]
19. Alenazi, N.A.; Hussein, M.A.; Alamry, K.A.; Asiri, A.M. Modified polyether-sulfone membrane: A mini review. *Des. Monomers Polym.* **2017**, *20*, 532–546. [[CrossRef](#)]
20. Rodrigo, G.; Gruvegard, M.; Van Alstine, J.M. Antibody fragments and their purification by protein L affinity chromatography. *Antibodies* **2015**, *4*, 259–277. [[CrossRef](#)]
21. Malpiedi, L.P.; Diaz, C.A.; Nerli, B.B.; Pessoa, A. Single-chain antibody fragments: Purification methodologies. *Process Biochem.* **2013**, *48*, 1242–1251. [[CrossRef](#)]
22. Cruz, A.R.; den Boer, M.A.; Strasser, J.; Zwarthoff, S.A.; Beurskens, F.J.; de Haas, C.J.C.; Aerts, P.C.; Wang, G.B.; de Jong, R.N.; Bagnoli, F.; et al. Staphylococcal protein A inhibits complement activation by interfering with IgG hexamer formation. *Proc. Natl. Acad. Sci. USA* **2021**, *118*, e2016772118. [[CrossRef](#)] [[PubMed](#)]
23. DeLano, W.L.; Ultsch, M.H.; de Vos, A.M.; Wells, J.A. Convergent solutions to binding at a protein-protein interface. *Science* **2000**, *287*, 1279–1283. [[CrossRef](#)] [[PubMed](#)]
24. Branco, R.J.; Dias, A.M.; Roque, A.C. Understanding the molecular recognition between antibody fragments and protein A biomimetic ligand. *J. Chromatogr. A* **2012**, *1244*, 106–115. [[CrossRef](#)] [[PubMed](#)]